



# Impact of Turning Parameters on AISI 420 Stainless Steel by CNC Machining

Saadat Ali Rizvi 

University Polytechnic, Jamia Millia Islamia, New Delhi, India  
sarizvil@jmi.ac.in, saritbhu@gmail.com

**Abstract.** The basic purpose of this study was to determine the impact of machining parameters on the surface roughness of AISI 420 martensitic stainless steel during the CNC turning and develop a mathematical model. AISI 420 martensitic stainless steel was selected for machining with precise vibration-less machinery. Rotational speed, feed rate, and depth of cut were considered as input parameters while surface roughness was set as an output parameter.  $L_{27}$  orthogonal array was used to optimize the process parameters, ANOVA was calculated and regression model was developed. Through the CNC machine, the idea of the near net shape manufacturing (NNM) can be possible through optimization of machining parameters. The rotational speed selected 1000, 1500, 2000 rpm and feed picked as 0.1, 0.2, 0.3 mm/rev and depth of cut were selected as 0.25, 0.45, and 0.65 mm for observation. The best parameters were obtained was at 1000 rpm, 0.65 mm depth of cut and 0.3 mm/rev is best machining parameter for surface roughness value.

**Keywords:** NNM, CLA, turning, martensitic stainless steel, surface roughness, mathematical model.

## 1 Introduction

The basic function of newer machining industries is to achieve the high degree of surface roughness of components. Quality (surface roughness) of a component is considerable important parameter in determining the productivity of turned parts and machine tool. Surface roughness [1] is an important parameter in assessment of mechanical properties and it can affect its performance. AISI 420 steel is well known as martensitic stainless steel which is frequently used to make the turbine blades due to its corrosion resistance properties [2-3] as chromium is in the main constituent from the range of 13-14% by weight and carbon up to 0.6%. As AISI 420 is a hard material hence turning of same is quite difficult [4]. Hard machining is referred as the machining of parts/components with a hardness of above 45HRC value. Lakhdar Bouzid et al [5] applied a RMS based optimization technique during the turning of AISI 420 SS to determine the surface roughness and they concluded that predicated value of surface

roughness is more closer that experimental. Hasan Basri Ulas and Murat Tolga Ozkan[6] applied an ANN technique to investigate the cutting forces during the machining of AISI 420 MSS and they found that cutting force modeled by ANN is very closer to experimental results. Lakhdar Bouzid et al [7] generated a mathematical model by RSM during the turning of AISI 420 MSS and they indicated in their result that feed rate is a parameter which highest affecting the surface roughness of AISI 420 MSS. bderrahmen Zerti et al [8] developed a model using RSM and ANN to assess the surface roughness of AISI 420 MSS during machining. They discovered that the feed rate significantly affects roughness. Additionally, it was shown that both ANN and RSM models aligned closely with experimental data, with ANN demonstrating superior accuracy. The optimal machining parameters for achieving multi-objective optimization are  $V_c=80$  m/min,  $f=0.08$  mm/rev, and  $a_p=0.141$  mm.S. Thamizhmanii et al [9] studied the roughness of martensitic stainless steel by turning process and they found that MSS (hard) materials are always advised to machining at medium level cutting speed, large feed rate, and large DOC. Sonu Mathew et al [10] studied the surface roughness of AISI 420MSS by EDM process and they concluded that the influence of current and pulse on time is crucial in EDM operations concerning surface roughness. It was found that to achieve lower surface roughness, the optimal settings for current, pulse on time, and pulse off time are 1A (level 1), 1.5  $\mu$ s (level 1), and 24  $\mu$ s (level 3), respectively. N. M. M. Reddy and P. K. Chaganti [11] try to optimize the SiO<sub>2</sub> during the turning of AISI 420 MSS and they mentioned in their result that Min. surface roughness was found at the machined surface of the AISI 402 for 1g of SiO<sub>2</sub> nanoparticles in base fluid, 150 m/min cutting speed, 0.15mm/rev feed and 0.1mm depth of cut.

## 2 Experimental design

### 2.1 Experimental set up

The experiments were conducted on a CNC lathe machine, of lokesh make 2-axis TL-20, swing diameter 300 mm, centre to centre distance 550 mm, spindle speed 4000 rpm and motor power of 10KW was selected for machining purpose. Carbide tool insert was considered as tool materials since the sharpness of cutting edge significantly affect the surface roughness of work piece.

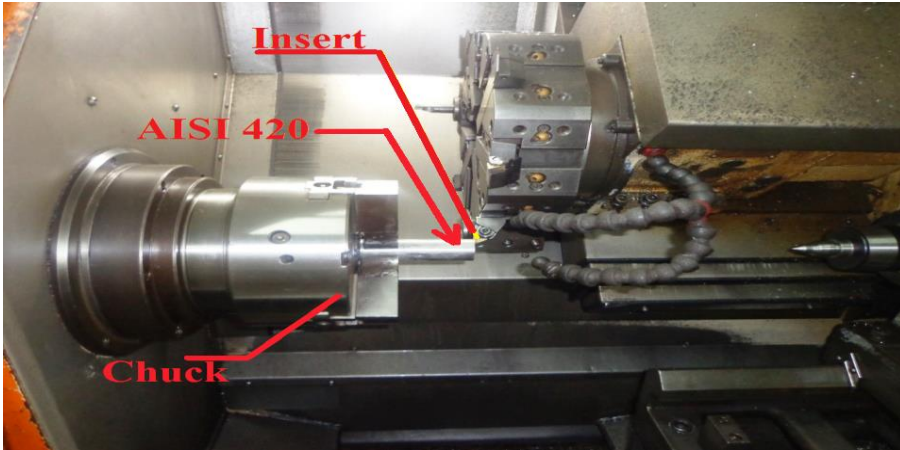


Fig. 1. Experimental setup

## 2.2 Process parameters

Three different speed, three different feed rate and three DOC were selected as process parameters and their respective values is listed in Table 1.

Table 1. Table captions should be placed above the tables.

Factor	Level		
Spindle speed (RPM)	1000	1500	2000
Feed rate (mm/min)	0.1	0.2	0.3
Depth of cut (DOC) mm	0.25	0.45	0.65

## 2.3 Material Used:

In this experimental work AISI420 martensitic stainless steel of  $\text{Ø } 25 \text{ mm} \times 100 \text{ mm}$  is used as work piece material. AISI 420 is a chromium-based steel which consist excellent corrosion resistance properties. It is hard but good ductility in the annealed condition but can be hardened up to 500 HB. It is difficult to machine. Cylindrical forms of work piece material were turned on CNC lathe machine without usage of any lubricant. Chemical composition of AISI 420 MSS is represented in the Table 2. It is widely used in making of nozzles, knives, surgical instruments, fasteners, shaft sleeves, spindles, shafts and plastic molds. The machining of AISI 420 was carried out with  $L_{27}$  orthogonal array with input process parameters. Surface roughness was considered as output parameter.

**Table 2.** Chemical Composition of AISI 420

S. N.	C	Mn	Si	S	P	Cr	Ni	Cu	Mo	Fe
1	0.32	0.72	0.25	0.018	0.019	12.10	0.18	0.04	0.04	Rest

**Fig. 2.** Samples after machined

### 3 Results and Discussion

After face turning and straight turning of all samples, roughness was measured with the help of Talysurf. Two surface roughnesses was measured one Arithmetic surface roughness ( $R_a$ ) and other is the highest peak to valley height ( $R_y$ ). Figure 2 shows work pieces after machined. The experiments have been conducted and the values of surface roughness for different combinations of spindle speed, feed rate, and depth of cut have been listed in Table 3.

**Table 3** Experimental Readings

S. No	Velocity	Feed (mm/rev)	Depth of Cut (mm)	$R_a$	$R_y$	S/N of $R_a$	Mean	S/N of $R_y$	Mean
1	1000	0.1	0.25	1.10	8.46	-0.8279	1.10	-18.5474	8.46
2	1000	0.1	0.45	1.18	8.73	-1.4376	1.18	-18.8203	8.73
3	1000	0.1	0.65	0.90	5.30	0.9151	0.90	-14.4855	5.30
4	1000	0.2	0.25	1.52	8.78	-3.6369	1.52	-18.8699	8.78
5	1000	0.2	0.45	1.35	6.01	-2.6076	1.35	-15.5775	6.01
6	1000	0.2	0.65	1.85	6.98	-5.3434	1.85	-16.8771	6.98
7	1000	0.3	0.25	2.99	14.40	-9.5134	2.99	-23.1672	14.40
8	1000	0.3	0.45	3.05	14.79	-9.6860	3.05	-23.3994	14.79
9	1000	0.3	0.65	3.07	15.42	-9.7428	3.07	-23.7617	15.42
10	1500	0.1	0.25	1.11	5.90	-0.9065	1.11	-15.4170	5.90
11	1500	0.1	0.45	1.54	7.68	-3.7504	1.54	-17.7072	7.68

12	1500	0.1	0.65	1.29	6.82	-2.2118	1.29	-16.6757	6.82
13	1500	0.2	0.25	1.21	6.85	-1.6557	1.21	-16.7138	6.85
14	1500	0.2	0.45	1.36	7.29	-2.6708	1.36	-17.2546	7.29
15	1500	0.2	0.65	1.33	7.47	-2.4770	1.33	-17.4664	7.47
16	1500	0.3	0.25	3.82	16.33	-11.641	3.82	-24.2597	16.33
17	1500	0.3	0.45	3.84	16.15	-11.686	3.84	-24.1635	16.15
18	1500	0.3	0.65	3.83	16.85	-11.664	3.83	-24.5320	16.85
19	2000	0.1	0.25	0.58	3.01	4.7314	0.58	-9.5713	3.01
20	2000	0.1	0.45	0.70	3.97	3.0980	0.70	-11.9758	3.97
21	2000	0.1	0.65	0.82	3.89	1.7237	0.82	-11.7990	3.89
22	2000	0.2	0.25	1.73	9.37	-4.7609	1.73	-19.4348	9.37
23	2000	0.2	0.45	1.64	8.37	-4.2969	1.64	-18.4545	8.37
24	2000	0.2	0.65	1.71	8.45	-4.6599	1.71	-18.5371	8.47
25	2000	0.3	0.25	3.68	17.23	-11.317	3.68	-24.7257	17.23
26	2000	0.3	0.45	3.55	16.03	-11.004	3.55	-24.0987	16.03
27	2000	0.3	0.65	3.58	16.95	-11.077	3.58	-24.5834	16.95

**3.1 Results and Graph variation of Taguchi optimization**

The experimental reading obtained from measurement of surface roughness is used to get the optimal cutting parameters with the help of Taguchi technique. (Fig 3 and 4)

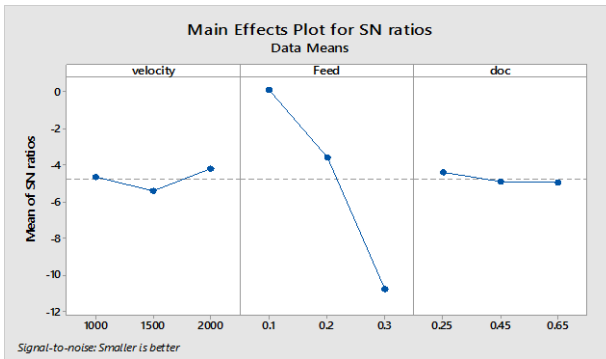


**Fig. 3.** S/N graph for surface roughness ( $R_a$ )

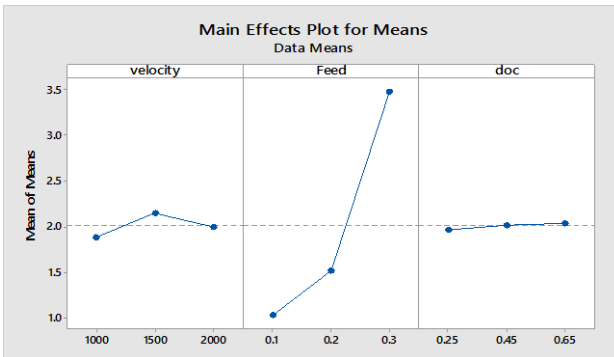


**Fig. 4.** Mean signal to noise graph for surface roughness ( $R_a$ )

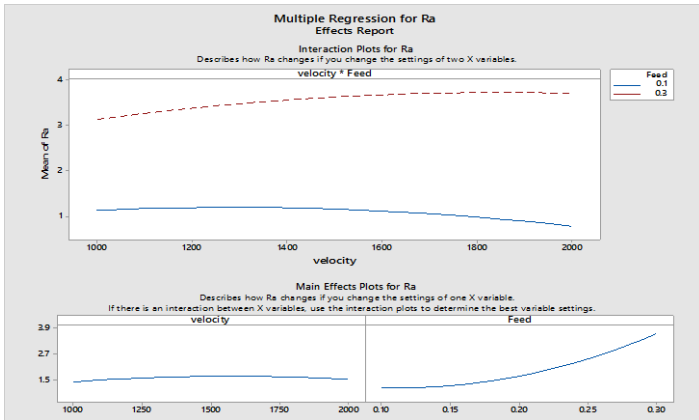


Fig. 5. Multiple Regression for  $R_a$  and interaction plots for  $R_a$

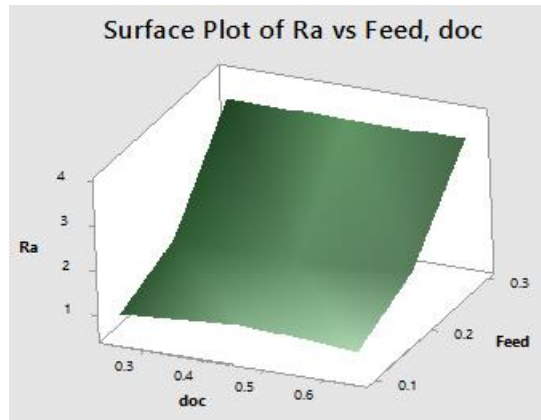


Fig. 6. Surface plot for surface roughness ( $R_a$ )

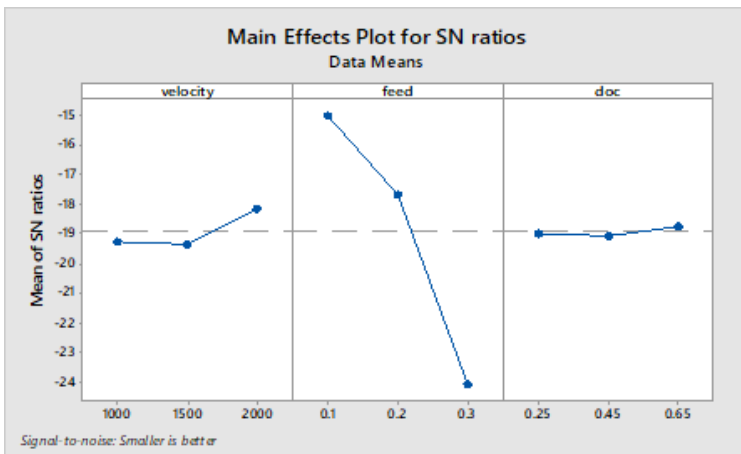


Fig. 7. S/N graph for surface roughness ( $R_y$ )

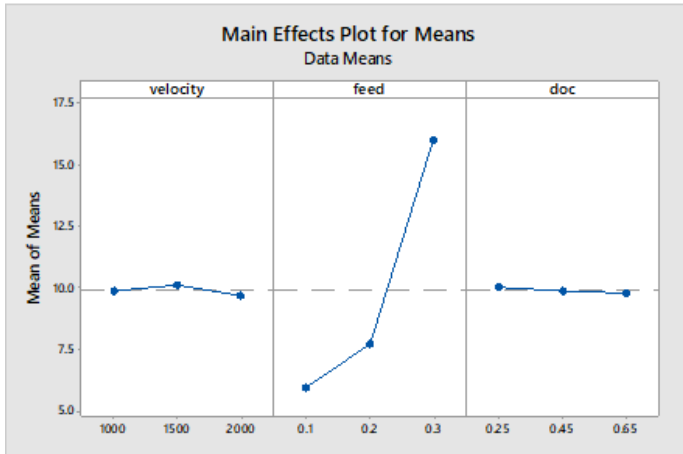


Fig. 8. Mean signal to noise graph for surface roughness ( $R_y$ )

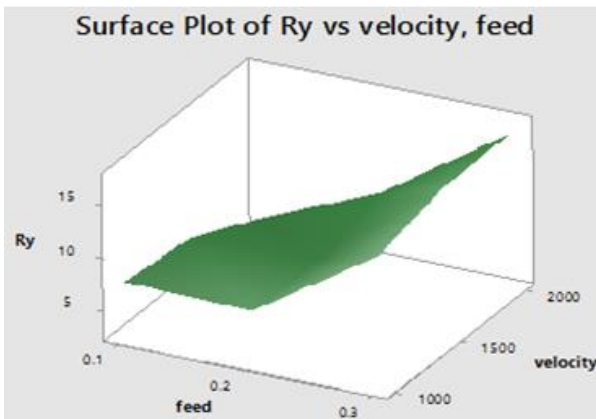


Fig. 9. Surface plot for surface roughness ( $R_y$ )

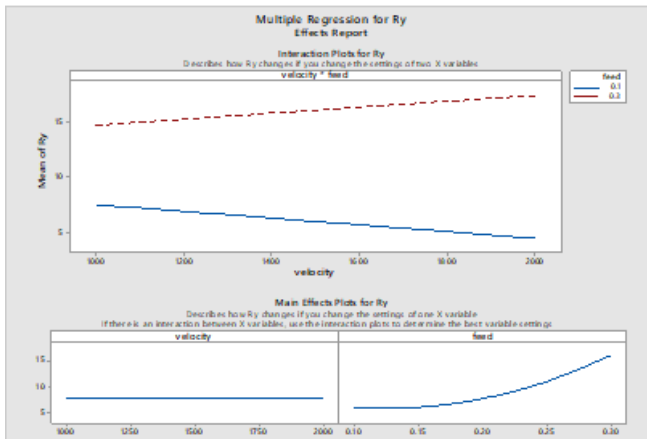


Fig. 10. Multiple Regression for  $R_a$  and interaction plots for  $R_y$

Fig 3 shows that the variation of the mean of S/N ratio with the velocity. Higher S/N ratio confirms to the optimal cutting condition. Fig 5 shows the interaction plot of speed and depth of cut. This shows how  $R_a$  changes if there is a change in the rotational speed or feed. Initially, surface roughness increases with increase in speed and then decreases keeping feed and depth of cut constant. Figures 6 and 7 illustrate the surface plots of  $R_a$  and  $R_y$ , demonstrating that an increase in feed rate leads to a rise in surface roughness. The depth of cut has minimal impact on surface roughness. Figure 10 presents the interaction plot for  $R_y$ , which also indicates that  $R_y$  increases with a higher feed rate. This section discusses the application of an orthogonal array to reduce the number of cutting trials for optimizing machining parameters. The results from the cutting experiments are analyzed using the S/N ratio and ANOVA. Based on these analyses, the optimal cutting parameter settings for surface roughness are determined and confirmed.

### 3.2 Analysis of S/N Ratio

In the Taguchi method, the term 'signal' refers to the desired value (mean) for the output characteristic, while 'noise' denotes the unwanted value (S.D.) for the output characteristic. Consequently, the S/N ratio is the proportion of the mean to the S.D. Taguchi employs the S/N ratio to assess how much the quality characteristic deviates from the target value. As previously mentioned, there are three types of quality characteristics: the-lower-the-better, the-higher-the-better, and the-nominal-the-better. To achieve optimal cutting performance, it is essential to apply the lower-the-better approach for surface roughness optimization. For the lower-the-better, the quality characteristic can be given by [12]

$$\frac{S}{N} = -10 \log \sum_{i=0}^n \frac{1}{y_i^2} \text{-----} \quad (1) \quad \text{higher the better}$$

$$\frac{S}{N} = -10 \log \frac{1}{n} \sum_{i=0}^n y_i^2 \text{-----} \quad (2) \quad \text{lower the better}$$

$$\frac{S}{N} = -10 \log \frac{1}{n} \sum_{i=0}^n (y_i - m)^2 \text{-----} \quad (3) \quad \text{normal the better}$$

In this context,  $n$  represents the number of tests, and  $y_i$  denotes the surface roughness value for the  $i^{\text{th}}$  test. Table 4 presents the experimental outcomes for surface roughness ( $R_a$ ) along with the corresponding S/N ratio calculated using Eq.2, while Table 5 displays measurements. Due to the orthogonal nature of the experimental design, it is feasible to isolate the impact of each cutting parameter at various levels. For instance, the average S/N ratio for cutting speed at levels 1, 2, and 3 can be determined by calculating the mean of the S/N ratios for experiments 1–9, 9–18, and 18–27, respectively. Similarly, the mean S/N ratio for each level of the other cutting parameters can be derived in the same way. The mean S/N ratio for each level of the cutting parameters is compiled and referred to as the S/N response table for surface roughness (Table 4). Additionally, the overall mean S/N ratio for all twenty-seven experiments is computed and included in Table 4. Figures 7 and 8 illustrate the S/N response graph for sur-

face roughness. As indicated in Eqs. (1) and (2), a higher S/N ratio corresponds to a smaller variance in tool life around the desired (the-higher-the-better) value. Nevertheless, understanding the relative significance of the cutting parameters for surface roughness is essential to determine the optimal combinations of cutting parameter levels. Tables 6 and 7 display the S/N ratio and mean value for surface roughness ( $R_y$ ).

**Taguchi Analysis:  $R_a$  versus Velocity, Feed, Depth of cut**

**Table 4.** Response table for the signal to noise ratio

Level	Spindle speed (rpm)	Feed rate (mm/min)	Depth of cut (mm)
1	-4.6533	0.1482	-4.392
2	-5.4071	-3.5676	-4.893
3	-4.1737	-10.814	-4.948
Delta	1.2334	10.963	0.556
Rank	2	1	3

**Table 5.** Response table for means

Level	Spindle speed (rpm)	Feed rate (mm/min)	Depth of cut (mm)
1	1.890	1.024	1.971
2	2.148	1.522	2.023
3	1.999	3.490	2.042
Delta	0.258	2.466	0.071
Rank	2	1	3

**Taguchi Analysis:  $R_y$  versus Velocity, Feed, Depth of cut**

**Table 6** Response table for the signal to noise ratio

Level	Spindle speed (rpm)	Feed rate (mm/min)	Depth of cut (mm)
1	-19.28	-15.0	-18.97
2	-19.35	-17.69	-19.05
3	-18.13	-24.08	-18.75
Delta	1.22	9.08	0.30
Rank	2	1	3

**Table 7.** Response table for means

Level	Spindle speed (rpm)	Feed rate (mm/min)	Depth of cut (mm)
1	1.890	1.024	1.971
2	2.148	1.522	2.023
3	1.999	3.490	2.042
Delta	0.258	2.466	0.071
Rank	2	1	3

### 3.3 Analysis of Variance

The aim of conducting an analysis of variance (ANOVA) is to determine which design input parameters have a significant impact on the quality characteristic [13]. This is achieved by dividing the overall variability of the S/N ratios, which is quantified by the sum of the squared deviations from the overall mean S/N ratio, into contributions from each design parameter and the error. Initially, the total sum of squared deviations SST from the overall mean S/N ratio is calculated as follows:

$$SS_{Total} = \sum_{i=0}^a \sum_{j=0}^b \sum_{k=0}^c y_{ijk}^2 - \frac{y_m^2}{abc} \dots\dots\dots(4)$$

$$SS_A = \frac{1}{bc} \sum_{i=0}^a y_{i.}^2 - \frac{y_m^2}{abc} \dots\dots\dots(5)$$

$$SS_B = \frac{1}{ac} \sum_{j=1}^b y_{.j}^2 - \frac{y_m^2}{abc} \dots\dots\dots(6)$$

$$SS_C = \frac{1}{ab} \sum_{k=1}^c y_{.k}^2 - \frac{y_m^2}{abc} \dots\dots\dots(7)$$

$$SS_{AB} = \frac{1}{c} \sum_{i=1}^a \sum_{j=1}^b y_{ij.}^2 - \frac{y_m^2}{abc} - SS_A - SS_B \dots\dots\dots(8)$$

$$SS_{BC} = \frac{1}{a} \sum_{j=1}^b \sum_{k=1}^c y_{.jk}^2 - \frac{y_m^2}{abc} - SS_B - SS_C \dots\dots\dots(9)$$

$$SS_{AC} = \frac{1}{b} \sum_{i=1}^a \sum_{k=1}^c y_{i.k}^2 - \frac{y_m^2}{abc} - SS_A - SS_C \dots\dots\dots(10)$$

$$SS_{Treatment} = SS_A + SS_B + SS_C + SS_{AB} + SS_{BC} + SS_{CA} \dots\dots(11)$$

The total sum of squared deviations,  $SS_T$ , is broken down into two components: the sum of squared deviations (SSD) attributed to each design parameter and the sum of squared error ( $SS_E$ ). The percentage contribution (P) of each design parameter to the total sum of squared deviations ( $SS_T$ ) is determined by the ratio of the sum of squared deviations ( $SS_D$ ) for each parameter to the total sum of squared deviations ( $SS_T$ ). Statistically, an F test, named after Fisher, is used to identify which design parameters significantly impact the quality characteristic. To conduct the F test, the mean of squared deviations ( $SS_M$ ) for each design parameter must be calculated. This mean is obtained by dividing the sum of squared deviations ( $SS_D$ ) by the degrees of freedom associated with the design parameter. The F value for each parameter is then calculat-

ed as the ratio of the mean of squared deviations ( $SS_M$ ) to the mean of squared error. Typically, an F value greater than 4 indicates that the change in the design parameter significantly affects the quality characteristic. An analysis of variance with arithmetic average roughness ( $R_a$ ) and  $R_y$  was conducted to examine the impact of cutting velocity ( $v$ ), feed ( $f$ ), and depth of cut ( $doc$ ) on the total variance of the result. Table 8 and Table 9 present the ANOVA results [14-15] for  $R_a$  and  $R_y$ , respectively. This analysis was performed with a 5% significance level, corresponding to a 95% confidence interval. The last column of the table displays the percentage contribution ( $p$ ) of each factor to the total variation, indicating its influence on the result. Based on the analysis of Table 8, it was clear that the feed rate (96%) [16], speed (0.95%), and the interaction between feed and speed (2.34%) significantly affect the resulting roughness  $R_a$ .

**Table 8.** Result of the analysis of variance (ANOVA) for surface roughness ( $R_a$ )

Sources of variation	Degree of freedom	Sum of square	Mean square	F	(%) Contribution
Speed	2	0.3015	0.15075	0.0772	0.95
Feed	2	30.597	15.2985	7.8353	95.9
Depth of cut	2	0.0245	0.01225	0.00627	0.08
Doc*feed	4	0.0982	0.02453	0.01256	0.155
Feed*speed	4	1.5138	0.3785	0.1938	2.385
Error	2	3.905	1.9525		0.53
Total	8	32.735		7.91877	100

**Table 9.** Result of the analysis of variance (ANOVA) for surface roughness ( $R_y$ )

Sources of variation	Degree of freedom	Sum of square	Mean square	F	(%) Contribution
Speed	2	0.938	0.469	0.0557	0.178
Feed	2	487.875	243.937	28.988	92.45
Depth of cut	2	0.277	0.1385	0.0165	0.052
Speed*feed	4	51.747	12.936	1.537	4.91
Feed*doc	4	5.818	1.454	0.1727	0.55
Doc*speed	4	14.71	3.678	0.437	1.41
Error		8.415			0.45
Total		569.78		31.355	100

In a similar manner, as seen in Table 9, the feed rate [16] factor significantly influences surface roughness ( $R_y$ ) with a contribution of 92.45%. Additionally, the interaction between speed and depth of cut accounts for 1.4%, while the interaction between feed and speed contributes 4.92%. Notably, the feed rate has the most substantial impact. Conversely, the depth of cut and speed do not significantly affect the surface roughness. The error calculated using the ANOVA table is 0.53% for surface roughness ( $R_a$ ) and 0.45% for surface roughness ( $R_y$ ).

### 3.4 Empirical modeling (Regression Analysis)

Several second-order regression equations have been applied to establish the relationship between machining parameters and the measured surface roughness. This model was created using Minitab-16 statistical software, and the resulting equation is as follows.

$$R_a = 1.529 + 0.00162 * \text{velocity} - 24.02 * \text{feed} - 0.000001 * \text{velocity}^2 + 73.50 * \text{feed}^2 + 0.00463 * \text{velocity} * \text{feed} + 0.01 * \text{doc}^2$$

$$R_y = 19.62 - 0.00592 * \text{velocity} - 123.4 * \text{velocity}^2 + 326.5 * \text{feed}^2 + 0.02870 * \text{velocity} * \text{feed}$$

### 3.5 Confirmation test

The confirmation test is conducted based on the information in Table 10. In this process, the authors randomly chose three combinations of cutting parameters and measured the surface roughness after the turning operation. This experimentally determined surface roughness is then compared to the roughness predicted by a mathematical model. The theoretical geometrical model [17] provides the arithmetic average surface roughness ( $R_a$ ) and the theoretical maximum peak to valley height ( $R_y$ ).

$$R_a = \frac{0.032f^2}{8r} \qquad R_y = \frac{f^2}{8r}$$

Where  $f$  is the feed in mm per revolution and  $r$  is the nose radius of the tool.

**Table 10.** Cutting condition used in a confirmation test

Test	Spindle speed (rpm)	Feed (mm/min)	Depth of cut (mm)
1	1200	0.15	0.30
2	1400	0.25	0.40
3	1600	0.35	0.50

**Table 11.** Confirmation trials and their comparison

Arithmetic surface roughness ( $R_a$ )					
Test	Exp	Theory	Error (%)	model	Error (%)
1	1.8	0.9	50	1.9	5.26
2	1.1	0.25	77.27	1.4	21.4

3	1.3	0.49	62.3	1.5	13.3
---	-----	------	------	-----	------

The confirmation table results indicate a comparison among the experimental value, the theoretical value, and the value derived from the mathematical model. This analysis reveals that the error is consistently smaller when the actual model is compared to the theoretical geometric model (Table 10 and 11).

## 4. Conclusion

In this study, the machining parameters for AISI 420 steel were optimized, and a mathematical model was developed. The turning experiments were conducted using an L27 orthogonal array. The findings are as follows:

The Taguchi method is the most effective and efficient approach for optimizing machining parameters related to surface roughness in turning.

The experimental results indicate that feed is the most critical factor among the three variables (feed, speed, and depth of cut) influencing the surface roughness of AISI 420 during machining.

The contribution of the depth of cut (DOC) to surface roughness is minimal.

For turning AISI 420, it is preferable to use high speed, slow feed, and low depth of cut. This method can improve surface roughness more effectively than relying on engineering judgments. According to ANOVA results, the feed rate and the interaction between feed rate and speed significantly contribute to surface roughness ( $R_a$ ) by 95.9% and 2.34, respectively. The experimental data suggest that a cutting speed of 1000 rpm, a feed rate of 0.3 mm/rev, and a depth of cut of 0.65 mm provide the optimal parametric conditions for machining AISI 420 MSS.

## References

1. Saadat Ali Rizvi, Wajahat Ali, Manufacturing Science – I by S.K. Kataria & Sons, New Delhi, 2013, 45-47
2. A. M. El-Tamimi, T. M. El-Hossainy, Investigating the Machinability of AISI 420 Stainless Steel Using Factorial Design, *Materials and Manufacturing Processes*, 23: 419–426, 2008. **DOI: 10.1080/10426910801974838**
3. Li Y, He Y, Xiu J, Wang W, Zhu Y, Hu B. Wear and corrosion properties of AISI 420 martensitic stainless steel treated by active screen plasma nitriding, *Surface and Coatings Technology*, 2017; 329:184-192
4. Noordin MY, Kurniawan D, Sharif S. Hard turning of stainless steel using wiper coated carbide tool, *International Journal of Preci Technology* 2007; 1: 75–84.
5. Lakhdar Bouzid, Mohamed Athmane Yallese, Salim Belhadi, Tarek Mabrouki, Lakhdar Boulanouar, RMS-based optimisation of surface roughness when turning AISI 420 stainless steel, *International Journal of Materials and Product Technology*, Vol. 49, No. 4, 2014, 224-251. **DOI: 10.1504/IJMPT.2014.064934.**
6. Ulas, Hasan Basri; Ozkan, Murat Tolga, Turning processes investigation of materials austenitic, martensitic and duplex stainless steels and prediction of cutting forces using artificial neural network (ANN) techniques, *Indian Journal of Engineering and Materials Sciences*, Vol.26(2), 2019, 93-104

7. Lakhdar Bouzid, Mohamed Athmane Yaltese<sup>1</sup>, Kamel Chaoui, Tarek Mabrouki, Lakhdar Boulanouar, Mathematical modeling for turning on AISI 420 stainless steel using surface response methodology, *Proceedings of the Institution of Mechanical Engineers, Part B: Journal of Engineering Manufacture*, 2014, 1-17, **DOI: [10.1177/0954405414526385](https://doi.org/10.1177/0954405414526385)**
8. Abderrahmen Zerti, Mohamed Athmane Yaltese, Oussama Zerti, Mourad Nouioua and Riad Khettabi, Prediction of machining performance using RSM and ANN models in hard turning of martensitic stainless steel AISI 420, *Proceedings of the Institution of Mechanical Engineers Part C Journal of Mechanical Engineering Science*, 2019, 1-24, **DOI: [10.1177/0954406218820557](https://doi.org/10.1177/0954406218820557)**
9. S. Thamizhmanii, B. Bin Omar, S. Saparudin, S. Hasan, Surface roughness analyses on hard martensitic stainless steel by turning, *Journal of Achievements of Materials and Manufacturing Engineering* 26(2), 2008, 139-142
10. Sonu Mathew, Deviprasad Varma P.R., Sabu Kurian P, Study on the Influence of Process Parameters on Surface Roughness and MRR of AISI 420 Stainless Steel Machined by EDM, *International Journal of Engineering Trends and Technology (IJETT)*, Vol.15 No.2, 2014, 54-58
11. N. M. M. Reddy, P. K. Chaganti, Investigating Optimum SiO<sub>2</sub> Nanolubrication During Turning of AISI 420 SS, *Engineering, Technology & Applied Science Research* Vol. 9, No. 1, 2019, 3822-3825.
12. Grzegorz Struzikiewicz, Andrzej Sioma, Evaluation of Surface Roughness and Defect Formation after The Machining of Sintered Aluminum Alloy AlSi10Mg, *Materials* 2020, 13(7), 1662, 1-13, **<https://doi.org/10.3390/ma13071662>**
13. Saadat Ali Rizvi, Application of Taguchi technique to optimize the GMA Welding parameters and study of fracture mode characterization of AISI 304H welded joints, *Int. Rev. Appl. Sci. Eng.* 9 (2018) 1, 9–16. **DOI: [10.1556/1848.2018.9.1.2](https://doi.org/10.1556/1848.2018.9.1.2)**
14. Amlana Panda, Ashok Kumar Sahoo, Isham Panigrahi, Arun Kumar Rout, Prediction models for on-line cutting tool and machined surface condition monitoring during hard turning considering vibration signal, *Mechanics & Industry* 21, 520 (2020), 1-16, **DOI: [10.1051/meca/2020067](https://doi.org/10.1051/meca/2020067)**
15. P.K. Swain, K.D. Mohapatra, R. Das, A.K. Sahoo, A. Panda, Experimental investigation into characterization and machining of Al+ SiCp nano-composites using coated carbide tool. *Mech. Ind.* 21, 307 (2020)
16. Oussama Zerti, Mohamed Athmane Yaltese, Riad Khettabi, Kamel Chaoui, Tarek Mabrouki, Design optimization for minimum technological parameters when dry turning of AISI D3 steel using Taguchi method, *International Journal of Advanced Manufacturing Technology* vol.89, 2017, 1915–1934. **doi.org/10.1007/s00170-016-9162-7**
17. Asutosh Panda, Sudhansu Ranjan Das, Debabrata Dhupal, Machinability investigation of HSLA steel in hard turning with coated ceramic tool, Assessment, modelling, optimization and economic aspects, *Journal of Advanced Manufacturing Systems* 18(4), 1-32, **DOI: [10.1142/S0219686719500331](https://doi.org/10.1142/S0219686719500331)**

**Open Access** This chapter is licensed under the terms of the Creative Commons Attribution-NonCommercial 4.0 International License (<http://creativecommons.org/licenses/by-nc/4.0/>), which permits any noncommercial use, sharing, adaptation, distribution and reproduction in any medium or format, as long as you give appropriate credit to the original author(s) and the source, provide a link to the Creative Commons license and indicate if changes were made.

The images or other third party material in this chapter are included in the chapter's Creative Commons license, unless indicated otherwise in a credit line to the material. If material is not included in the chapter's Creative Commons license and your intended use is not permitted by statutory regulation or exceeds the permitted use, you will need to obtain permission directly from the copyright holder.

